Hindawi
Advances in Materials Science and Engineering
Volume 2019, Article ID 2187132, 7 pages
https://doi.org/10.1155/2019/2187132

Research Article

Synthesis of Magnetic Biochar for Efficient Removal of Cr(III) Cations from the Aqueous Medium

Liliya Frolova[1] **and Mykola Kharytonov**[2]

[1]*Department of Inorganic Materials Technology and Ecology, University of Chemical Technology, Dnipro 49005, Ukraine*
[2]*Department of Soil Science and Farming, Dnipro State Agrarian and Economic University, Dnipro 49600, Ukraine*

Correspondence should be addressed to Liliya Frolova; 19kozak83@gmail.com

Received 29 January 2019; Revised 2 March 2019; Accepted 17 March 2019; Published 1 April 2019

Academic Editor: Michael J. Schutze

Porous biochars obtained from coniferous woods, and magnetic biochars based on them, which showed high sorption properties when extracting Cr(III) from aqueous solutions (from 0.005 to 0.0125 mol/L), were studied. The adsorption properties of the magnetic biochar are compared with the initial biochar. It has been established that the preparation of materials by the method of pyrolysis and subsequent treatment in a plasma reactor makes it possible to bring the samples under study into a number of promising adsorbents for the extraction of chromium from aqueous solutions.

1. Introduction

Chromium and its compounds are widely used in various industries. This is based on its valuable properties such as heat resistance, hardness, and corrosion resistance. As an alloying additive, chromium is used for smelting various grades of steel and alloys, which are used in the engineering, aviation, and space industries. Chromium oxides are the raw material for the preparation of polishing pastes and paints for glass and ceramics and are part of chromium-containing catalysts. Chromium salts are used in the production of anticorrosive pigments and electroplating [1–4]. All these technological processes lead to the formation of a large amount of concentrated wastewater. Chromium(III) compounds, especially chromium(VI), are toxic to humans and animals [5].

There are many effective technologies for the treatment of chromium-containing wastewater such as chemical precipitation, electrochemical, and membrane [6–8]. However, there are no universal methods for removing chromium from wastewater. The chromium content in various wastewater varies in the range from 5–10 to 3000–5000 mg/l. Large volumes of solutions, a large variety of related impurities, and high content of chromium make it difficult to process them to extract chromium.

The application of sorption technologies is promising. In recent years, research in the field of adsorption technologies has shown interesting results for the treatment of concentrated wastewater from the industry. Today, adsorbents have been synthesized to remove heavy metal cations, including highly dangerous inorganic and organic substances [6, 9–11].

The advantages of adsorption technologies are simple hardware design, high degree of purification, and simple methods of regeneration of used adsorbents. Widely used adsorbents based on activated carbons, zeolites, silica gel, and active metal oxides have a high cost. Currently, many researchers are developing technologies for obtaining new cheap adsorbents or chemosorbents, which are not inferior in efficiency to industrial analogs [12–16].

There are a number of works [17–27] related to the study of the possibility of using wastes as adsorbents. Plant waste as adsorbents is an attractive option because of their low cost and large quantities. However, these types of adsorbents have common drawback. They are difficult to separate from the solution, which increases operating costs. Magnetic materials can be used to solve this problem. Magnetic composite adsorbents can combine the rapid and efficient separation of suspensions with high adsorption activity [28, 29].

In this paper, we propose obtaining a composite magnetic biochars based on biochar of coniferous trees, studying its properties, checking its adsorption abilities, and comparative analysis of its adsorption properties with precursors (magnetite and biochar).

2. Materials and Methods

The biochar of coniferous species of wood, the composite magnetic adsorbent based on biochar of coniferous species, was used as adsorbents.

Pyrolysis of the biomass was carried out in an electric shaft-type laboratory furnace. A sample of biomass was loaded into a cylindrical retort, which was placed in an oven. After that, the furnace was heated to a predetermined temperature. The biomass was processed at a temperature of 700°C. The pyrolysis time was determined by the final processing temperature of the biomass. The residue obtained after pyrolysis was dry extinguished until completely cooled.

For the synthesis of magnetic sorbents, $FeSO_4 \cdot 7H_2O$ and NaOH (analytical grade) were used. Magnetite was obtained by chemical precipitation from an aqueous solution of ferrous sulphate with sodium hydroxide with subsequent treatment in a plasma reactor [30]. The resulting suspension was separated on a magnetic filter and dried at a temperature of 150°C for 2 hours. The composite adsorbent was prepared similarly, but magnetite was deposited on the surface of the biochar.

X-ray phase analysis of the samples was carried out on a DRON-2 diffractometer (DRON-2.0, Co-Kα-radiation). The mode of operation of the X-ray source is 40 kV, 30 mA. The range of scan angles is 2θ from 10 to 90°. The morphology of the surface of the sorbent is determined using a JSM-6390LV scanning electron microscope (JEOL, Japan).

Fourier-transform infrared spectroscopy (FT-IR) was also used to analyze adsorbents before and after adsorption of Cr(III). Spectra were obtained in the range from 400 to 4000 cm^{-1} using a Fourier-transform infrared spectra spectrometer (FT-IR, Nicolet 6700, Thermo Fisher Scientific, USA).

In order to study transformations, thermal differential analysis and differential thermogravimetric (DTG) analysis are used. DG curves and TG curves were recorded on derivatograph Q-1500D (F. Paulik, J. Paulik, and L. Erdey). Temperature was varied in a range of 20–850°C at a heating rate of 10 deg/min. α-Al_2O_3 was used as a reference. Mass of each sample was 200 mg. The biochars were subjected to XRD analyses with diffractometer DRON-2 with Co_α-radiation to obtain the structural properties.

The sorption properties of the samples were calculated by determining the degree of sorption of chromium(III) cations of different initial concentrations (0.0125, 0.01, and 0.005 mol/L). The amount of adsorbent in model solutions also varied from 0.5–1.5 g/10 ml. The contact time was 300 s.

The chromium concentration was determined spectrophotometrically using a UV 5800 PC spectrometer.

The degree of sorption was calculated by reducing the concentration of chromium cations in an aqueous solution according to the following formula:

$$\%S = \frac{(C_0 - C_t) \cdot 100\%}{C_0}, \quad (1)$$

where C_0 is the initial concentration of chromium(III) in solution (mg/L) and C_t is the concentration of chromium(III) in the solution at the moment of time t (mg/L).

The equilibrium sorption capacity q_e (mg/g) was calculated by the following equation:

$$q_e = \frac{(C_0 - C_e) \cdot V}{m}, \quad (2)$$

where C_0 is the initial concentration of chromium(III) in solution (mgl/L), C_e is the equilibrium concentration (mgl/L), V is the volume of solution (ml), and m is the mass of the adsorbent (g).

The study consisted in performing several series of experiments with biochar based on coniferous breeds of BC wood and magnetic biochar BM.

In some cases, the properties of BC after adsorption of cations Cr(III) were studied.

3. Results and Discussion

3.1. X-Ray Diffraction Analysis. At the first stage, the phase composition of the biochar was investigated. As can be seen from X-ray diffractograms (Figure 1), this is an amorphous substance consisting of silicates of magnesium, calcium carbonate, and silicon oxide. It can be assumed that it is the amorphous structure and the complex chemical composition that provide a high adsorption capacity. Biochars before and after adsorption of cations Cr(III) have similar diffractograms. However, some small differences were noted among the samples. In sample 2 (Figure 1(b)), additional peaks appear, corresponding to chromium sulphate, and the intensity of all base peaks is almost two times lower than that of the original sample. Small unexpressed peaks indicate the presence of inorganic components such as SiO_2, $CaCO_3$, and K_2MgSiO_4.

On X-ray diffraction patterns of MB, a pronounced crystal structure of magnetite is visible, and an amorphous phase is present. All peaks have a higher intensity than BC.

3.2. FT-IR Spectroscopy. FT-IR spectra and spectroscopic investigation of a biochar before and after adsorption are shown in Figures 2(a) and 2(b). Different bands in the spectra represented oscillations of a low intensity of functional groups in biochars [31]: –OH (3700–3250 cm^{-1}). Very intense corresponding C-O-C ethers (1310–100 cm^{-1}), C=C aromatic rings (1525–1475 cm^{-1}) and C=O (1615 cm^{-1}), aromatic CO- and phenolic–OH (1480 cm^{-1}), C-OC (1057 cm^{-1}), and nitropics (N=O) at 1680–1450 cm^{-1} and =C-H peak around 870 cm^{-1}. A broad peak at 1500–1630 cm^{-1} is associated with the presence of lignin.

The bands responsible for stretching the O–H and C=O groups disappear after sorption of Cr(III). Therefore, it can be stated that, first of all, carboxyl and hydroxyl groups are involved in the sorption of cations. It can be seen from Figure 2(b) that the position of the –OH groups peak varies

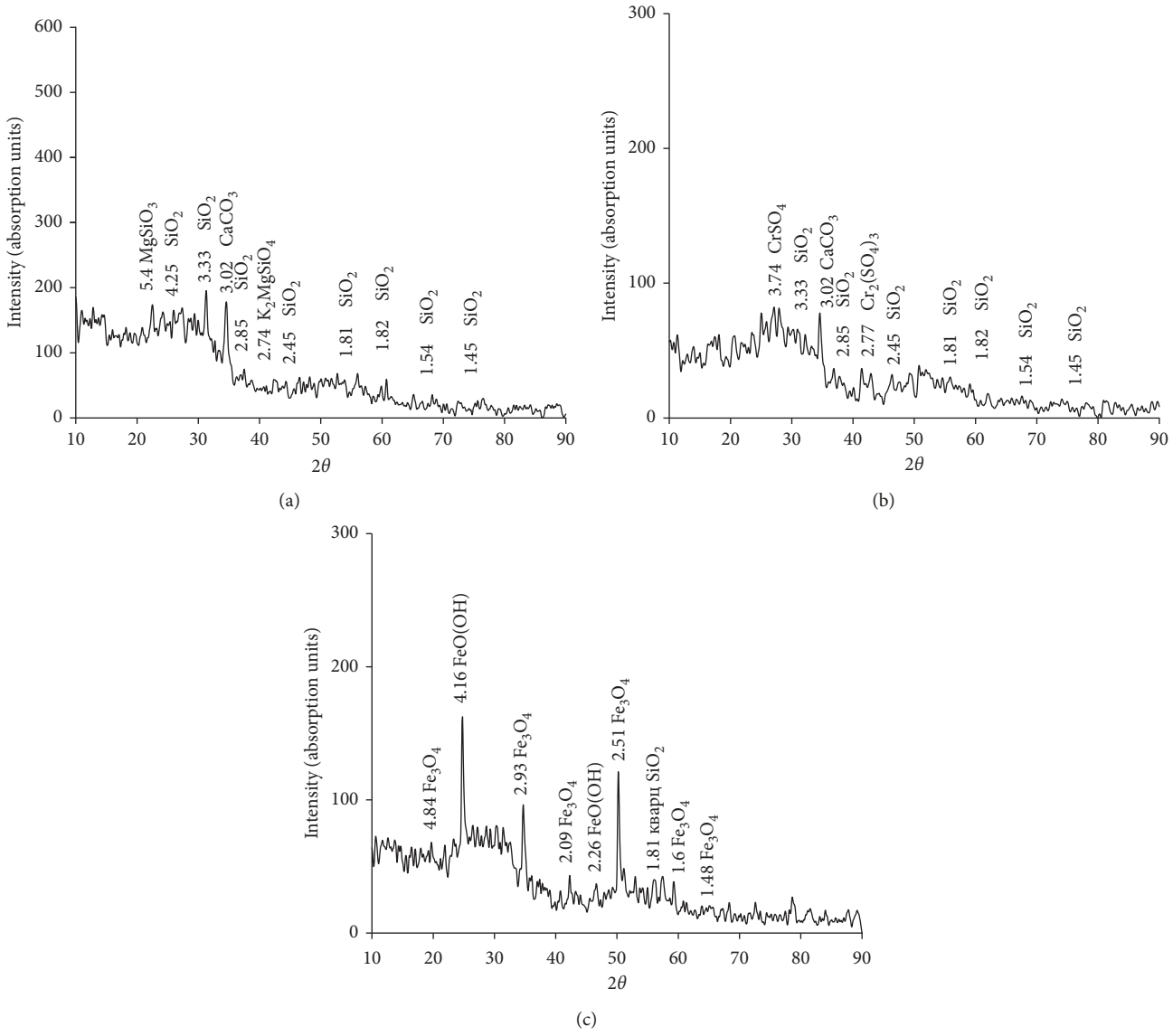

Figure 1: X-ray diffraction patterns of (a) biochar BC, (b) biochar BC after adsorption of cations Cr(III), and (c) MB.

from 3148 cm^{-1} to 3384 cm^{-1} after the sorption process. This observation may indicate a complex biochar structure with phenol groups on the surface during sorption. In addition, peaks appear in the range of 1225–980 cm^{-1}, corresponding to the S=O and S–O shaft group at 870–690 cm^{-1}.

The FT-IR spectra of MB (Figure 2(c)) have many peaks in the shortwave region corresponding to the Fe–O bonds. The presence of intense peaks of the corresponding –OH groups (3700–3250 cm^{-1}) is observed.

3.3. Thermogravimetric Analysis. The results of thermogravimetric analysis are shown in Figure 3. All three derivatograms have a similar appearance. Adsorbents have a high mass loss for biochars, and the percentage of mass loss is 31.6, for the spent adsorbent 34.8 and for magnetic biochar 40.1. From the DTG curves, it can be seen that the maximum rate of mass loss is observed at a temperature of 100–175°C, which is associated with the release of bound water. There is a slight exoeffect associated with the decomposition of cellulose at a temperature of about 380°C for biochar. Wide peaks from 450 to 500°C are associated with decomposition of residual and refractory lignin. In the high-temperature region, additional peaks appear, corresponding to the removal of sul groups.

3.4. Scanning Electron Microscopy (SEM). The study of the surface structure of BC and MB showed (Figure 4) the presence on the surface of large deep pores. The developed microstructure was observed in all adsorbents. The formation of large pores is associated with the presence in conifers of a large amount of resinous substances, hemicellulose, cellulose, and lignin, which, at a high temperature of pyrolysis, partially ferment, which contributes to the formation of stable large pores. Such a structure provides high

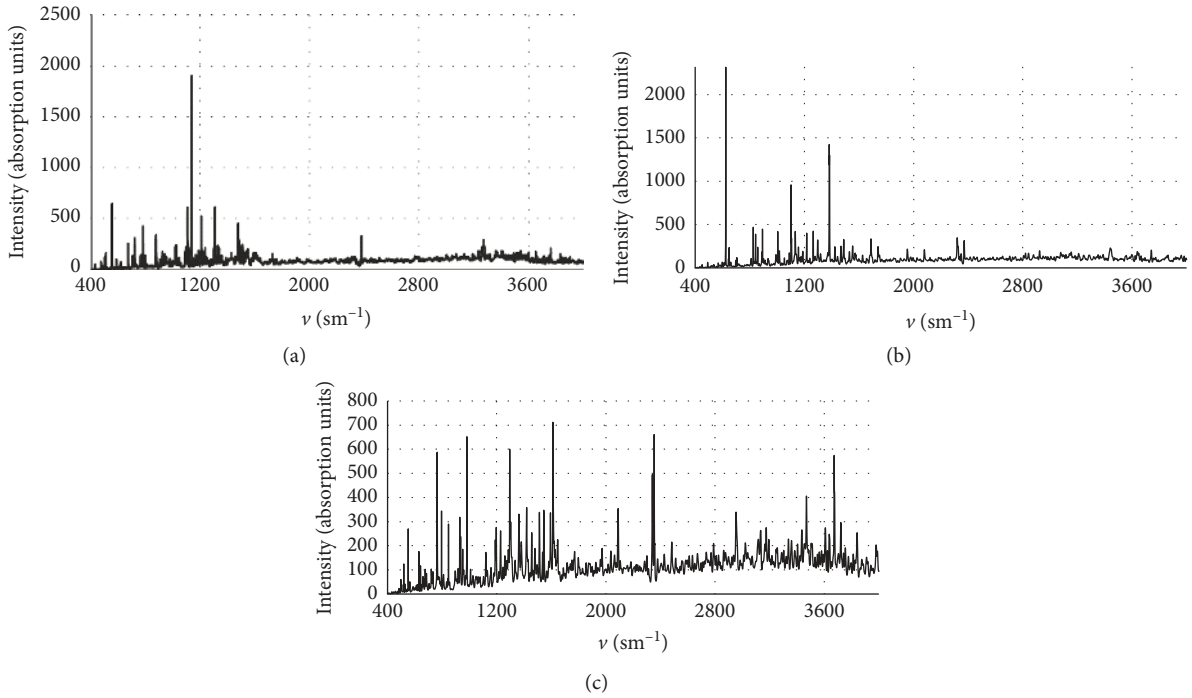

Figure 2: IR spectra of BC (a), spent biochar BC after adsorption of Cr (III) (b), and MB (c).

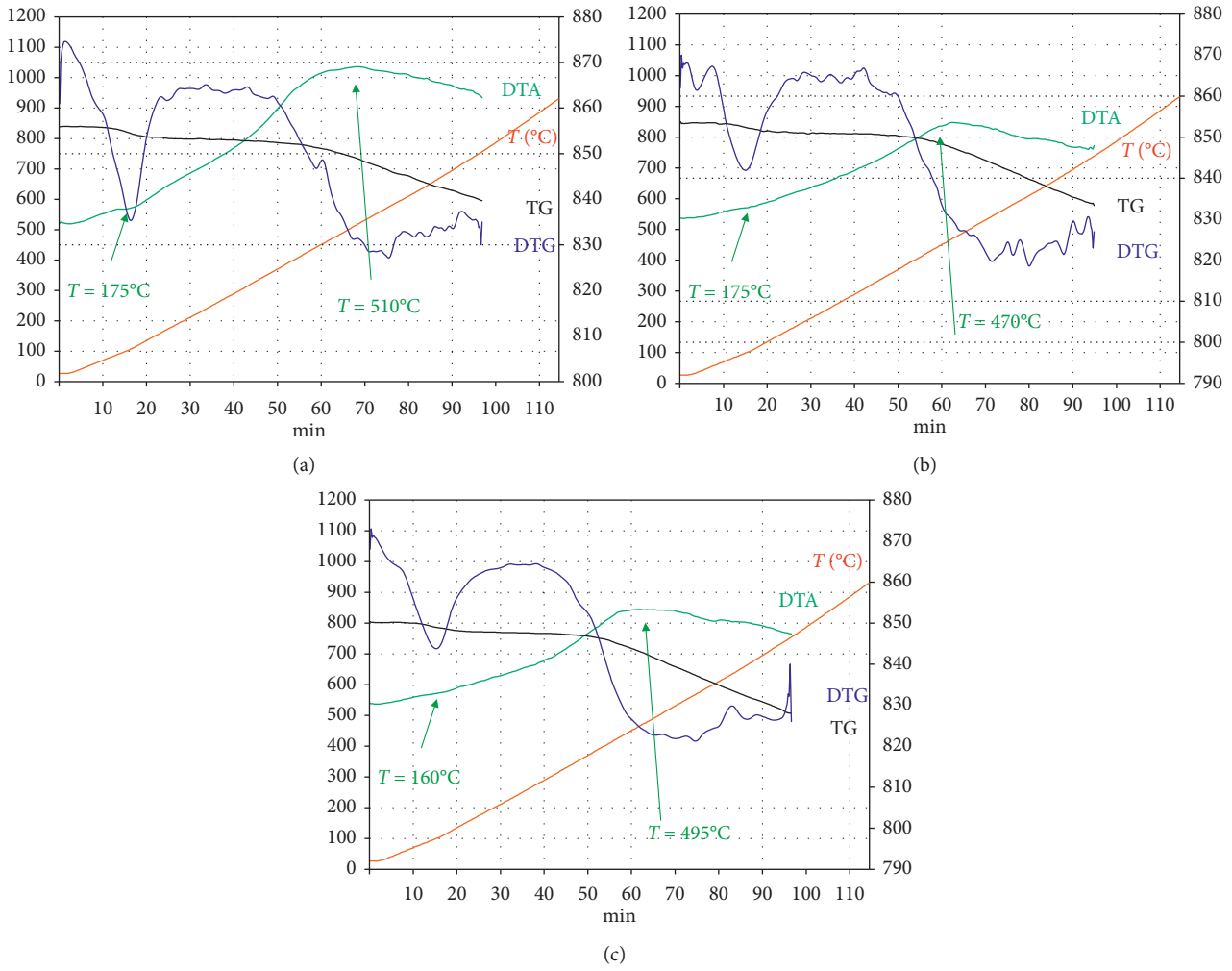

Figure 3: Derivatograms of adsorbents: BC (a), spent biochar BC after adsorption of Cr(III) (b), and MB (c).

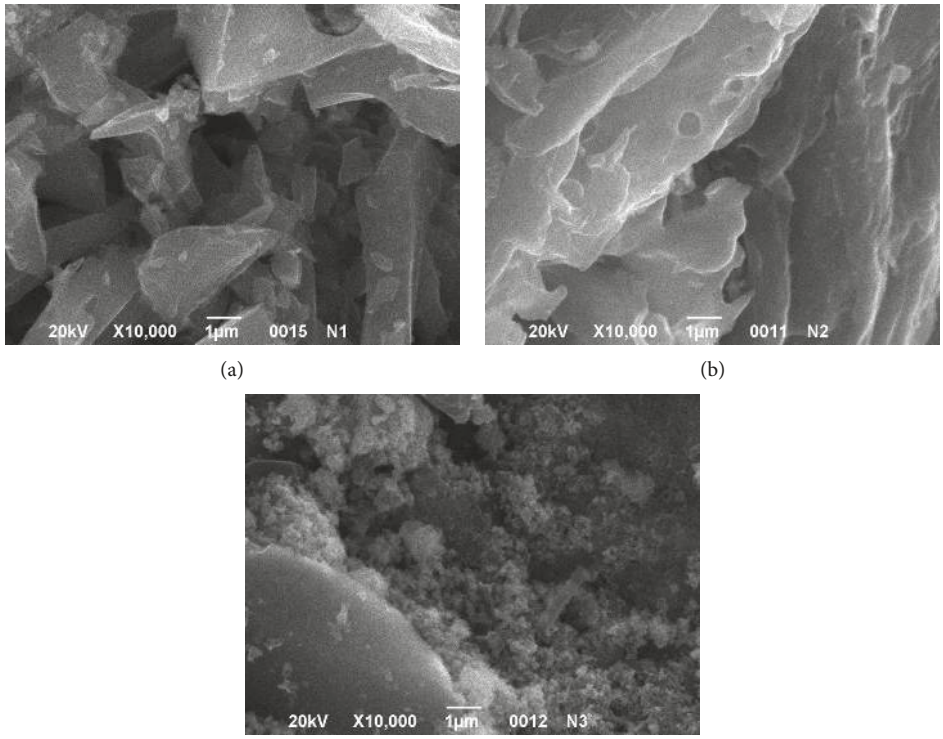

(a) (b) (c)

Figure 4: SEM images of adsorbents: BC (a), spent biochar BC after adsorption of Cr(III) (b), and MB (c).

adsorption properties of BC. This is confirmed by microphotographs of biochar after adsorption. Its structure without pronounced pores is apparently due to their filling with chromium cations.

Magnetic biochar shows a well-developed porosity and uniform distribution of pores along its surface. The formation of nanodispersed oxide phases on the surface of cavities and pores leads to an increase in the specific surface and the creation of new spaces. Increasing the number of pores provides a large surface area and high adsorption capacity.

3.5. Magnetic Properties. Figure 5 shows the magnetization curves for magnetic biochars and magnetite, recorded at room temperature. The magnetic biochar produced by the plasma method showed ferromagnetic properties, which are characterized by a coercive force of 51 Oe and a saturation magnetization of 20 Emu/g (for magnetite, $H_c = 5$ Oe, $M = 82$ Emu/g).

3.6. Sorption Experiment. The dose of the adsorbent is an important factor that should be considered for the effective removal of Cr(III) cations, since it determines the equilibrium in the system [4]. The results of the adsorption experiments are shown in Figures 6–8 for degree adsorption (%) and sorption capacity (mg/g). The amount of adsorption decreases with increasing dose of the adsorbent. On the other hand, the percentage of adsorption increases first with an increase in the amount of the adsorbent and reaches

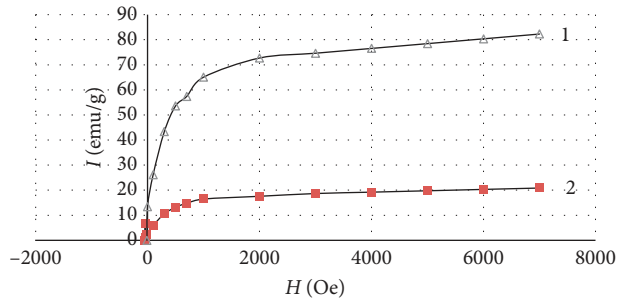

Figure 5: Magnetic measurements of 1: magnetite and 2: magnetic biochar.

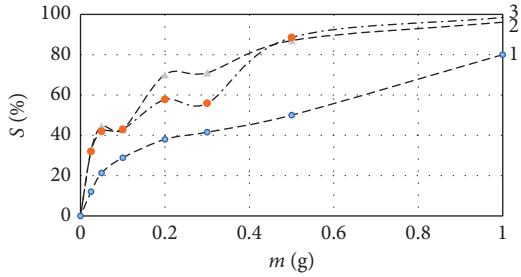

Figure 6: Dependence degree of the adsorption on the mass on the adsorbent 1: 0.0125, 2: 0.01, and 3: 0.005.

saturation. The initial increase in the percentage of adsorption can be explained by an increase in the surface area of the biochar and the presence of a larger number of active

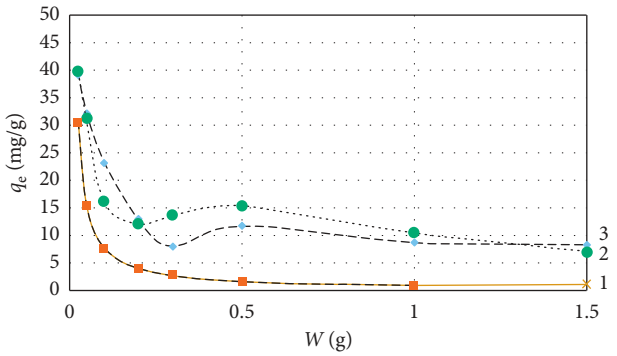

Figure 7: Dependence of the adsorption capacity of chromium(III) on the mass biochar 1: 0.0125, 2: 0.01, and 3: 0.005.

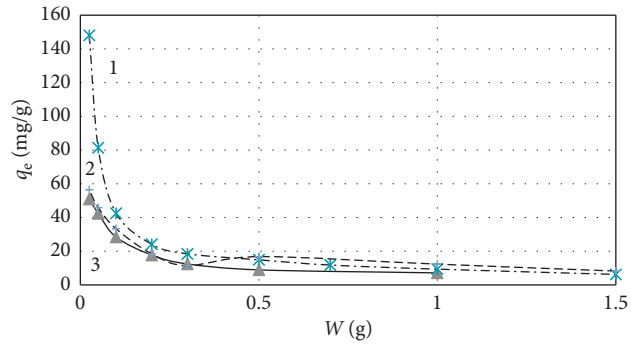

Figure 8: Dependence of the adsorption capacity of chromium(III) on the mass of the adsorbent 1: magnetic biochar, 2: biochar, and 3: magnetite, $C = 0.0125$ mol/L.

adsorption sites. A decrease in the intensity of adsorption can be associated with the achievement of limiting adsorption and an increase in the value in the denominator (formula (1)), as a result of which the overall result decreases. In accordance with the results of further periodic experiments on adsorption, an adsorbent dose of 0.5 g was chosen for Cr(III) with a contact time of 300 seconds. Taking into account the value of q_e, the capacity of the magnetic biochar is 150 mg/g.

The maximum percentage removal was about 99% that reached a maximum with 1.0 and 1.5 g of the adsorbent for both CB and MB (Figure 8).

Possible reactions can take place with different cations:

$$\begin{aligned}
CaO + H_2O &\longrightarrow Ca(OH)_2 \\
MgO + H_2O &\longrightarrow Mg(OH)_2 \\
Cr_2(SO_4)_3 + 3Ca(OH)_2 &\longrightarrow 3CaSO_4 \\
&\quad + 2Cr(OH)_3 \\
Cr_2(SO_4)_3 + 3Mg(OH)_2 &\longrightarrow 3MgSO_4 \\
&\quad + 2Cr(OH)_3 \\
3K_2MgSiO_4 + 2Cr_2(SO_4)_3 + 21H_2O &\longrightarrow Cr_4(SiO_4)_3 \\
&\quad + 3[MgSO_4 \cdot 7H_2O] \\
&\quad + 3K_2SO_4 \\
Ca_3SiO_5 + Cr_2(SO_4)_3 + 6H_2O &\longrightarrow Cr_2SiO_5 \\
&\quad + 3[CaSO_4 \cdot 2H_2O]
\end{aligned} \tag{3}$$

For the magnetic biochar, the degree of purification reaches 98–100%. The degree of purification from chromium cations decreases with an increase in the concentration of the initial chromium solution from 0.005 mol/L to 0.0125 mol/L. The magnetic biochar is of greater capacity than magnetite and biochar.

4. Conclusions

A new magnetic biochar was successfully synthesized using a coniferous biochar using plasma processing. The results showed the high efficiency of the magnetic adsorbent combining the high adsorption capacity of the initial biochar with magnetite magnetic properties. The prepared magnetic biochar showed a wide network of pores due to the dispersed magnetite on the surface.

The magnetic biochar showed high magnetic characteristics of coercivity 50 Oe and saturation magnetization 40 Emu/g.

The Cr(III) removal ability varies from 32 ± 0.5 mg/g of the biochar to 140 ± 0.5 mg/g for the magnesium biochar at an initial range of concentrations of Cr(III) of 0.0125, 0.01, and 0.005 mol/L. As can be seen from their IR spectra, functional OH groups on the surface of the biochar promote adsorption.

The mechanism of adsorption of Cr(III) by a biochar mainly includes the chemisorption process and cations attached to the biochain matrix. It can be also explained with the significant adsorption capacity of a magnetic biochar that combines a developed and hydrated surface.

Data Availability

For commentary, FT-IR spectra used a literary source, which is available at http://www.fulviofrisone.com/attachments/article/406/Infrared%20and%20Raman%20Spectroscopy%20-%20Methods%20and%20Applications.pdf. This preliminary study is cited in the appropriate place in the text as a reference [31].

Conflicts of Interest

The authors declare that they have no conflicts of interest.

Acknowledgments

The research and publication of the article was supported with the Ministry of Education and Science of Ukraine.

References

[1] S. Karamchedu, E. Hryha, and L. Nyborg, "Changes in the surface chemistry of chromium-alloyed powder metallurgical steel during delubrication and their impact on sintering," *Journal of Materials Processing Technology*, vol. 223, pp. 171–185, 2015.

[2] K. Binnemans and P. T. Jones, "Solvometallurgy: an emerging branch of extractive metallurgy," *Journal of Sustainable Metallurgy*, vol. 3, no. 3, pp. 570–600, 2017.

[3] R. Galindo, C. Gargori, N. Fas, M. Llusar, and G. Monrós, "New chromium doped powellite (Cr-$CaMoO_4$) yellow ceramic pigment," *Ceramics International*, vol. 41, no. 5, pp. 6364–6372, 2015.

[4] L. Verger, O. Dargaud, M. Chassé, N. Trcera, G. Rousse, and L. Cormier, "Synthesis, properties and uses of chromium-based pigments from the Manufacture de Sèvres," *Journal of Cultural Heritage*, vol. 30, pp. 26–33, 2018.

[5] Z. C. Ayturan, F. Kunt, and S. Dursun, "Metal bioaccumulation/toxicity test for metal industry wastewaters," *International Journal of Environmental Pollution and Environmental Modelling*, vol. 1, no. 1, pp. 1–5, 2018.

[6] A. Subramani and J. G. Jacangelo, "Emerging desalination technologies for water treatment: a critical review," *Water Research*, vol. 75, pp. 164–187, 2015.

[7] Z. Zhao, B. Zhang, D. Chen, Z. Guo, and Z. Peng, "Simultaneous reduction of vanadium(V) and chromium(VI) in wastewater by nanosized $ZnWO_4$ Photocatalysis," *Journal of Nanoscience and Nanotechnology*, vol. 16, no. 3, pp. 2847–2852, 2016.

[8] O. N. Tsybulskaya, T. V. Ksenik, A. A. Yudakov, and V. V. Slesarenko, "Reagent decontamination of liquid chrome containing industrial wastes," *Environmental Technology and Innovation*, vol. 13, pp. 1–10, 2019.

[9] O. Sahu, B. Mazumdar, and P. K. Chaudhari, "Treatment of waste water by electrocoagulation: a review," *Environmental Science and Pollution Research*, vol. 21, no. 4, pp. 2397–2413, 2014.

[10] S. S. Tahir and R. Naseem, "Removal of Cr(III) from tannery waste water by adsorption on to bentoniteclay," *Separation and Purification Technology*, vol. 53, no. 3, pp. 312–321, 2007.

[11] L. Frolova and A. Pivovarov, "Obtaining of brown pigments from concentrated wastewater containing nickel," *Chemistry & Chemical Technology*, vol. 10, no. 2, pp. 209–212, 2016.

[12] L. A. Frolova, A. A. Pivovarov, T. E. Butyrina, and E. G. Tsepich, "Purification of waste waters containing chromium by a sorbent based on blast furnace slag," *Journal of Water Chemistry and Technology*, vol. 37, no. 4, pp. 185–190, 2015.

[13] O. D. Uluozlu, A. Sari, M. Tuzen, and M. Soylak, "Biosorption of Pb(II) and Cr(III) from aqueous solution by lichen (*Parmelina tiliaceae*) biomass," *Bioresource Technology*, vol. 99, no. 8, pp. 2972–2980, 2008.

[14] D. H. K. Reddy and Y. S. Yun, "Spinel ferrite magnetic adsorbents: alternative future materials for water purification," *Coordination Chemistry Reviews*, vol. 315, pp. 90–111, 2016.

[15] A. Downie, A. Crosky, and P. Munroe, "Physical properties of biochar," in *Biochar for Environmental Management: Science and Technology*, pp. 13–32, Earthscan, London, UK, 2009.

[16] M. I. Inyang, B. Gao, Y. Yao et al., "A review of biocharas a low-costad sorbent for aqueous heavy metal removal," *Critical Reviewsin Environmental Science and Technology*, vol. 46, no. 4, pp. 406–433, 2016.

[17] J.-H. Park, Y. S. Ok, S.-H. Kim et al., "Competitive adsorption of heavy metal sontose same straw biochar inaqueous solutions," *Chemosphere*, vol. 142, pp. 77–83, 2016.

[18] J. Komkiene and E. Baltrenaite, "Biochar asad sorbent for removal of heavy metal ions [Cadmium(II), Copper(II), Lead(II), Zinc(II)] from aqueou sphase," *International Journal of Environmental Science and Technology*, vol. 13, no. 2, pp. 471–482, 2016.

[19] C. Rumpel, J. Leifeld, C. Santin, and S. Doerr, "Movement of biochar in the environment," in *Biochar for Environmental Management: Science, Technology and Implementation*, p. 907, Taylor & Fransis, Abingdon, UK, 2015.

[20] H. Lyu, Y. He, J. Tang et al., "Effect of pyrolysis temperature on potential toxicity of biochar if applied to the environment," *Environmental Pollution*, vol. 218, pp. 1–7, 2016.

[21] Y. Yuan, N. Bolan, A. Prévoteau et al., "Applications of biochar in redox-mediated reactions," *Bioresource Technology*, vol. 246, pp. 271–281, 2017.

[22] A. Ahmed, J. Kurian, and V. Raghavan, "Biochar influences on agricultural soils, crop production, and the environment: a review," *Environmental Reviews*, vol. 24, no. 4, pp. 495–502, 2016.

[23] E. Moreno-Jiminez, J. M. Fernández, M. Puschenreiter, P. N. Williams, and C. Plaza, "Availability and transfer to grain of As, Cd, Cu, Ni, Pb and Zn in a barley agri-system: impact of biochar, organic and mineral fertilizers," *Agriculture, Ecosystems & Environment*, vol. 219, pp. 171–178, 2016.

[24] Y. Han, X. Cao, X. Ouyang, S. P. Sohi, and J. Chen, "Adsorption kinetics of magnetic biochar derived from peanut hull on removal of Cr(VI) from aqueous solution: effects of production conditions and particle size," *Chemosphere*, vol. 145, pp. 336–341, 2016.

[25] Y. Deng, T. Zhang, and Q. Wang, "Biochar adsorption treatment for typical pollutants removal in livestock wastewater: a review," in *Engineering Applications of Biochar*, InTech, London, UK, 2017.

[26] H. Li, X. Dong, E. B. da Silva, L. M. de Oliveira, Y. Chen, and L. Q. Ma, "Mechanisms of metal sorption by biochars: biochar characteristics and modifications," *Chemosphere*, vol. 178, pp. 466–478, 2017.

[27] C. Peiris, S. R. Gunatilake, T. E. Mlsna, D. Mohan, and M. Vithanage, "Biochar based removal of antibiotic sulfonamides and tetracyclines in aquatic environments: a critical review," *Bioresource Technology*, vol. 246, pp. 150–159, 2017.

[28] F. Reguyal, A. K. Sarmah, and W. Gao, "Synthesis of magnetic biochar from pine sawdust via oxidative hydrolysis of $FeCl_2$ for the removal sulfamethoxazole from aqueous solution," *Journal of Hazardous Materials*, vol. 321, pp. 868–878, 2017.

[29] K. R. Thines, E. C. Abdullah, N. M. Mubarak, and M. Ruthiraan, "Synthesis of magnetic biochar from agricultural waste biomass to enhancing route for waste water and polymer application: a review," *Renewable and Sustainable Energy Reviews*, vol. 67, pp. 257–276, 2017.

[30] L. A. Frolova and M. P. Derhachov, "The effect of contact non-equilibrium plasma on structural and magnetic properties of $Mn_XFe_{3-X}O_4$ spinels," *Nanoscale Research letters*, vol. 12, no. 1, pp. 505–517, 2017.

[31] B. Schrader, *Infrared and Raman Spectroscopy: Methods and Applications*, John Wiley & Sons, Hoboken, NJ, USA, 2008.